Article

Testing and application of a two-dimensional hydrothermal/transport model for a long, deep, and narrow lake with moderate Burger number

Rakesh K Gelda,[1] Alexandra T. King,[2] Steven W. Effler,[1]* Seth A. Schweitzer,[2] and Edwin A. Cowen[2]

[1] *Upstate Freshwater Institute, NY, USA*

[2] *DeFrees Hydraulics Laboratory, School of Civil and Environmental Engineering, Cornell University, Ithaca, NY, USA*

** Corresponding author: sweffler@upstatefreshwater.org*

Received 17 October 2014; accepted 13 July 2015; published 9 October 2015

Abstract

Setup, testing, and application of a 2-dimensional longitudinal–vertical hydrothermal/transport model (the transport submodel of CE-QUAL-W2) was documented for Cayuga Lake, New York, where the Rossby radius is on the order of the lake's width. The model was supported by long-term monitoring of meteorological and hydrologic drivers and calibrated and validated using in-lake temperature measurements made at multiple temporal and spatial scales over 16 years. Measurements included (1) temperature profiles at multiple lake sites for 10 years, (2) near-surface temperatures at one end of the lake for 16 years, (3) high frequency temperature at multiple depths for 2 years, and (4) seasonal measurements of a conservative passive tracer. Seiche activity imparted prominent signatures within these measurements. The model demonstrated excellent temporal stability, maintaining good performance in uninterrupted simulations over a period of 15 years. Performance was improved when modeling was supported by on-lake versus land-based meteorological measurements. The validated model was applied through numeric tracer experiments to evaluate various features of transport of interest to water quality issues for the lake, including (1) residence times of stream inputs within the entire lake and a smaller region defined bathymetrically as a shallow shelf, (2) transport and fate of negatively buoyant streams, and (3) the extent of transport from the hypolimnion to the epilimnion. This hydrothermal/transport model is appropriate to serve as the transport submodel for a forthcoming water quality model for this lake and for other high aspect (length to width) ratio lacustrine systems for which the internal Burger number is order one or greater.

Key words: Burger number, calibration, lake, model, Rossby radius, seiche, thermal stratification, transport, 2-dimensional, validation

Introduction

Temperature is a fundamental regulator of the physical character of water and thereby the ecology and quality of surface waters because it structures biological communities and affects the rates of biochemical processes (Wetzel 2001). Seasonal thermal stratification is ubiquitous in deep, temperate lakes and reservoirs and is an important regulator of transport processes (Imboden 2004). The critical dependence of lake metabolism and related metrics of water quality on stratification and associated transport regimes has been widely acknowledged (e.g., Lam and Schertzer 1987, Wetzel 2001, Imboden 2004). Water motion and features of stratification in lakes and reservoirs depend on a number of factors, including basin morphometry, setting, hydrology, and meteorological conditions (Csanady 1973, Imboden 1990, 2004, Imberger 1994). Internal seiches (successive oscillations of stratified layers) are particularly prominent features of water motion in long, narrow (high aspect ratio) lakes (Hunkins and Fliegel 1973, Lemmin and Mortimer 1986), promoting turbulence and thus vertical

DOI: 10.5268/IW-5.4.804

© International Society of Limnology 2015

transport (Gloor et al. 1994, MacIntyre and Jellison 2001, Wüest and Lorke 2003). Substantial year-to-year variations in stratification and transport occur in response to natural variations in hydrologic and particularly meteorological drivers (Effler et al. 1986, Rueda and Cowen 2005, Gelda and Effler 2007a, O'Donnell et al. 2010).

A number of mechanistic mathematical models, ranging from averaged or integrated forms of the Navier-Stokes equations coupled to an equation of state and various scalar transport equations (e.g., Rueda and Cowen 2005) to parameterized mass-conserving dynamic 1-dimensional (1-D) box models (e.g., Imberger and Patterson 1981), have been developed to simulate the dynamics of the thermal stratification and transport regimes of lakes and reservoirs (e.g., Martin and McCutcheon 1999, Hodges et al. 2000, Boegman et al. 2001). Moreover, tested mechanistic stratification/transport models serve as the physical frameworks (e.g., transport submodel) for mass balance water quality models (Chapra 1997, Martin and McCutcheon 1999), quantifying the interplay between these physical attributes and features of water quality. The primary differences in these models are the number of spatial dimensions represented (Martin and McCutcheon 1999), including 1-D (vertical layers; e.g., Imberger and Patterson 1981, Owens et al. 2013), 2-dimensional (2-D, vertical layers and longitudinal segments: e.g., Gelda and Effler 2007a; or depth-averaged and horizontally resolved: e.g., Cheng et al. 1993), and 3-dimensional (3-D; Hodges et al. 2000, Rueda and Cowen 2005) frameworks. Multiple, often system-specific, factors influence the selection of an appropriate framework, including (1) the water quality modeling principle of parsimony (adopting a framework only as complex as necessary to address the issue; Chapra 1997, Martin and McCutcheon 1999), (2) the temporal and spatial scales of interest, (3) observed spatial patterns in both physical and water quality characteristics, and (4) computational demands. Each of the dimensional alternatives can have limitations based on these considerations.

Model testing for a broad range of drivers, and for an array of measured variables, is desired to establish robustness and credibility (Gelda and Effler 2007a, O'Donnell et al. 2010, 2011). Natural tracers, such as specific conductance (O'Donnell et al. 2011) and conservative ions (Martin and McCutcheon 1999), can support testing of the simulation of transport and fate of streams. Fixed-frequency collections of vertically detailed temperature profiles support testing of performance for the simulation of the features of the seasonal stratification regime. High frequency temperature measurements collected at multiple depths using thermistor chains resolve signatures of water motion to test model performance related to seiche activity (Horn et al. 1986, Lemmin and Mortimer 1986).

Many lakes and reservoirs have high aspect ratio (e.g., length ÷ width) configurations, where seiche activity is a prominent feature of transport, and differences in water quality are primarily a concern along the longitudinal rather than the lateral dimension (Martin and McCutcheon 1999). A 2-D laterally averaged transport model with vertical layers and longitudinal segments may be an appropriate and parsimonious selection for many high aspect ratio lacustrine systems. The objectives of this study were to (1) demonstrate the robust testing of such a 2-D hydrothermal/transport model for a high aspect ratio, deep lake (Cayuga Lake, NY); and (2) consider its appropriateness for this and other high aspect ratio systems. Model testing was based on comparisons of model predictions with measured (1) fixed-frequency vertical temperature profiles for 10 years, (2) signatures of oscillations in stratified layers and intrusions of hypolimnetic waters into surface layers (upwelling events) from high frequency temperature measurements for multiple years, and (3) signatures of tributary entry to both upper and stratified layers from a passive tracer. The validated model was applied to describe and quantify features of transport that have implications with respect to water quality modeling, including residence time of stream inputs, transport and fate of inflowing streams, and exchange between the hypolimnion and epilimnion.

System description

Cayuga Lake (42°41′30″N, 76°41′20″W) is the fourth easternmost of the 11 New York Finger Lakes (Fig. 1) and has the second largest surface area (172 km^2) and volume (9.4×10^9 m^3). The mean and maximum depths are 55 m and 133 m, respectively. This long and narrow system has an aspect ratio (length to width) of 22 (11, if maximum width is used) and is positioned along a north-northwest–south-southeast axis that coincides with prominent wind directions (Fig. 1, see wind rose). Cayuga Lake has a warm monomictic stratification regime, stratifying strongly in summer through mid-fall, but only rarely developing complete ice cover (Oglesby 1978). Barotropic seiches (i.e., basin-scale standing waves on the water surface), baroclinic seiches (i.e., basin-scale standing waves within the metalimnion), internal waves (oscillations in and across stratified layers at a broad range of length and time scales), and upwelling events occur in the lake in response to wind energy inputs, promoted by its elongated shape and the prevailing wind directions (Effler et al. 2010). The potential for rotation (Coriolis acceleration) modifying baroclinic motion is described by the Burger number (S; Antenucci and Imberger 2001, Antenucci 2005):

$$S = \frac{c}{Lf}, \quad (1)$$

© International Society of Limnology 2015 DOI: 10.5268/IW-5.4.804

where c is the wave celerity in a non-rotating system, L is a length scale characterizing the lake width, and f is the Coriolis parameter. The value of S ranges from 0.4 to 1.9 in Cayuga Lake, with maximum values in August and September and lower values in May and October when stratification is weaker. If the lake were well-mixed (i.e., a continuously stirred tank reactor [CSTR]; Rueda et al. 2006), residence time (and flushing time) could be determined by dividing the lake volume by the total volumetric inflow rate (V/Q). Based on an annual average total volumetric inflow rate of 30.8 m^3 s^{-1} (1987–2013 average), the CSTR-based residence time estimate is 8.2 y.

Cayuga Lake is a phosphorus (P)-limited mesotrophic lake (Oglesby 1978, Effler et al. 2010). Nearly 40% of the total tributary inflow to the lake, as well as 3 point-source discharges, enter its southern end. Large quantities of sediment (Effler et al. 2010), P (Prestigiacomo et al. 2014), and dissolved color (Effler et al. 2015) are delivered to the southern end of the lake by the tributaries during runoff events. A shallow region, designated "the shelf," with a maximum depth of 6 m extends 1.6 km from the southern end of the lake before a sharp drop-off in depth (Fig. 1). Conditions on the shelf have generally been considered degraded relative to the pelagic zone (Oglesby 1978, Effler et al. 2010, 2014). Monitoring since the late 1990s has established that 2 trophic state metrics, the concentration of total P and Secchi depth, are significantly higher and lower, respectively, on the shelf compared with pelagic waters, although chlorophyll *a* concentrations (widely adopted as a metric of phytoplankton biomass) did not follow a similar trend (Effler et al. 2010), at times being lower on the shelf. A mechanistic P-eutrophication model is to be developed for the entire lake to provide a quantitative framework to support management deliberations, including the feasibility of improving conditions on the shelf relative to pelagic regions.

Dreissenid mussels invaded the lake in the mid-1990s, originally zebra mussels (Watkins et al. 2012). Quagga mussels subsequently became dominant, with substantial population densities throughout the water column, but particularly through metalimnetic depths (Watkins et al. 2012). A spatially intensive survey of population densities in 2013 (Watkins and others, unpubl. data) found levels that matched or exceeded those observed for Lake Erie (MacIsaac et al. 1992) and Lake Michigan (Nalepa et al. 2014), where substantial related impact on lake metabolism was reported. Such populations of this bivalve play potentially important roles for the P-eutrophication issue, as a sink for phytoplankton and a P recycling pathway (Boegman et al. 2008a, 2008b), mediated through filter feeding (Wong et al. 2014) and excretion (Bootsma and Liao 2014), respectively. The effects of mussel metabolism will likely be integrated into the forthcoming P-eutrophication model (e.g., Boegman et al. 2008b, Zhang et al. 2008).

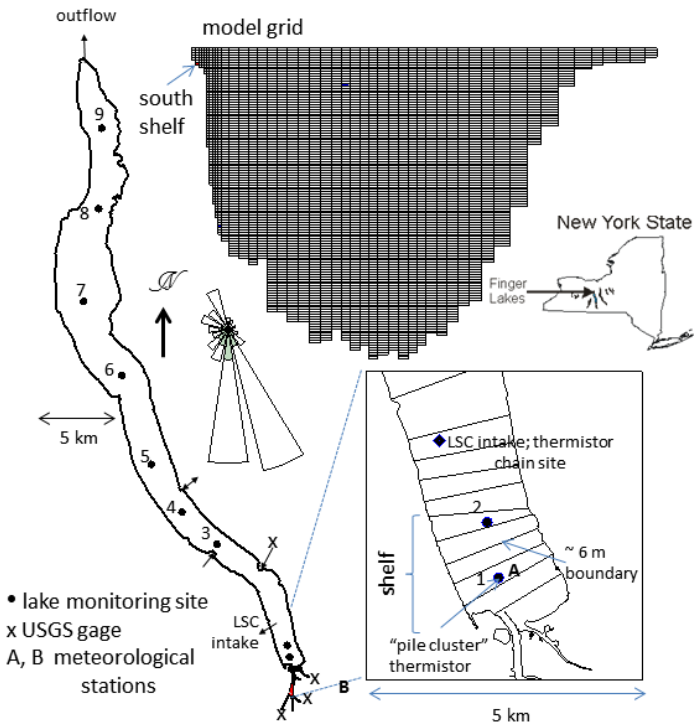

Fig. 1. Cayuga Lake, location within New York, positions of inflows and outflows, and sites of hydrologic, meteorological, and lake monitoring. Enlarged map of shelf, and wind rose (data from site A; May–Oct 2013) included. Model grid of lake consisting of longitudinal sediments and vertical (1 m thick) layers.

Methods

Model description

The 2-D hydrothermal/transport model adopted in this study, henceforth called W2/T, serves as the transport submodel of the water quality model CE-QUAL-W2. This dynamic model is based on the finite difference solution in the vertical and longitudinal dimensions of laterally and layer-averaged equations for momentum, mass, and heat conservation, governing 6 unknown fields: horizontal and vertical components of velocity, free surface position, hydrostatic pressure, water temperature, and density (Edinger and Buchak 1975, Chung and Gu 1998, Gu and Chung 1998, Cole and Wells 2013). Surface heat exchange was calculated using an explicit term-by-term process to represent the effects of evaporative heat loss, short- and long-wave radiation, convection, conduction, and back radiation (Cole and Wells 2013). The model provides a range of options for simulating vertical turbulent transport process. Both the mixing–length model with Richardson correction and the *k-ε* (turbulent kinetic energy/dissipation) model alternatives were tested. The former was less computationally expensive and performed better; hence, it was used for all simulations reported herein.

W2/T represents the lake with a grid of longitudinal segments divided into vertical layers (Fig. 1). Cell boundaries are fixed in space. The geometry of the computational grid is determined by the boundaries, the average cross-sectional (lateral) widths of the longitudinal segments, and thicknesses of the vertical layers. Meteorological inputs (drivers) for the model include wind speed and direction, air temperature (T), dew point T, and incident solar radiation. Values of the light attenuation coefficient for irradiance (K_d, m^{-1}; downwelling), which quantifies the vertical limit of the penetration of solar energy in the water column, need to be specified. Volumetric inflow rate, inflow T (for heat budget and density/buoyancy), and volumetric outflow rate must also be specified. The model has 6 coefficients that may be adjusted in the calibration process (Table 1).

Model specifications, development of inputs, and supporting data

Cayuga Lake was represented by 48 longitudinal segments and 132 layers of 1 m thickness (3720 total cells), consistent with the guidelines of Cole and Wells (2013). The average segment length was 375 m at the southern end that includes the shelf (10 segments). The average segment length for the remainder of the lake was 1355 m. Morphometric features of the grid were based on the bathymetric analysis of Vandebroek (2011). Inflows directly enter model segments for the 5 largest tributaries (together 60% of the total) and 4 point-source inputs (2 municipal waste effluents and 2 cooling water operations with subsurface intakes; Fig. 1). The remaining 40% of tributary inflow associated with about 20 small streams (Haith et al. 2012) was input as "distributed" inflows (uniformly around the lake perimeter).

Table 1. Two-dimensional hydrothermal/hydrodynamic model (W2/T) calibration coefficient values for Cayuga Lake, NY.

Coefficient	Value
longitudinal eddy viscosity	1 $m^2\ s^{-1}$
longitudinal eddy diffusivity	1 $m^2\ s^{-1}$
Chezy coefficient	70 $m^{0.5}\ s^{-1}$
wind sheltering coefficient	1.0
fraction of incident solar radiation absorbed at the water surface	0.45
coefficient of bottom heat exchange	7.0×10^{-8} W $m^{-2}\ s^{-1}$

There were 2 sources of meteorological inputs (Table 2a). One monitoring station is located on a piling cluster within the southern shelf (site A, Fig. 1) and recorded measurements every 10 min from October 2011 through 2013. The other is land-based site B, proximate to the shelf (Fig. 1), and recorded measurements hourly (1 hour is the most common time step for W2/T inputs; Cole and Wells 2013). Site A measurements proved best as model drivers but were not available before October 2011; hence, we used simultaneous wind measurements from sites A and B to find the best fit linear transform for predicting site A velocities from site B velocities. A different set of best-fit coefficients were found for each 45° wind velocity sector (for site B). The best-fit transform was used to predict site A velocities from site B velocities when site A measurements were not available.

Estimates of volumetric inflow were based on continuous gauge measurements (US Geological Survey) for 4 of the largest tributaries (~50% of the watershed). Inflows from ungauged streams were prorated according to watershed area. Area weighting of inflow was supported for Cayuga Lake by earlier success in modeling long-term trends for a conservative substance using this method (Effler et al. 1989).

Paired vertical profiles of irradiance (E), specific conductance (SC), and T were collected biweekly at 2 or more pelagic sites over the April–October interval of 1998–2006 and 2013 (Table 2b). Values of K_d were determined from the E profiles according to Beer's Law (Kirk 2011) and linearly interpolated to obtain daily estimates. Measurements of SC (a passive tracer) in the lake and the largest tributaries in 2013 provided a test of model representation of tributary inflow fate. A large and diverse

© International Society of Limnology 2015 DOI: 10.5268/IW-5.4.804

Table 2. Monitoring data, model drivers, lake signatures.

(a) Meteorological data*

Location (see Fig. 1)	Interval	Frequency
A "piling cluster"	27 Oct 2011–31 Dec 2013	10 min (missing data filled-in with Ithaca Airport data)
[+]B Cornell University	1987–2013	hourly

* air T, dewpoint T, wind speed, wind direction, and solar radiation; see Fig. 1 for locations
[+] wind speed data were adjusted to the measurements at location A

(b) Lake Data

Type	Location[x]	Interval	Comments
T (Sea-Bird SBE-39), E, and SC[+]; vertical profiles	sites 2, 3 and LSC intake	1998–2006	0.25 m vertical resolution, bi-weekly, Apr–Oct; accuracy ±0.002 °C
	sites 1–9	2013	as above, but weekly at 3 sites
T; 2 m depth (YSI 6560)	site 2	2013	frequency 1 h, Apr–Oct; accuracy ±0.15 °C
T; near-surface (Stowaway, TBI32)	site A	1998–2012	frequency 10 min–1 h, Apr–Oct; accuracy ±0.002 °C
T; thermistor chain (every 4.5–5 m in ~70 m of water) (Sea-Bird SBE-39)	LSC intake	2012, 2013	Apr–Oct, frequency 1 min, accuracy ±0.002 °C

[x] see Fig. 1 for locations
[+] T = temperature, E = irradiance, SC = specific conductance

dataset of lake T measurements (Table 2b) supported robust testing of the model's performance with respect to both hydrothermal and transport characteristics. Spectral analyses of the thermistor chain observations at multiple depths were conducted (e.g., Lemmin and Mortimer 1986) to identify characteristic periods of internal waves.

Execution, testing, performance evaluation, and model applications

Model calibration was conducted for 2013, the year with the most T measurements, using the (bi)weekly vertical T profiles from sites 1–9 (Table 2b). The set of model coefficients (Table 1) established in calibration were retained for validation, which employed T observations of all frequencies from all sites and years (Table 2). Simulations for the validation years were year-round and continuous for 1998–2012 (i.e., there was no re-initialization of the model within individual years). The model's ability to predict tributary inflow fate was tested using SC as a passive tracer. The initial model SC of the lake for early April of 2013 was established from measurements at site 3. Model stream inputs of SC over the subsequent April to early August interval were specified by stream measurements of SC to support prediction of lake vertical profiles of SC for early August.

Model performance with respect to T was evaluated both qualitatively and quantitatively. Prominent features of stratification (e.g., upwelling and internal seiche timing, vertical dimensions, and temperatures of layers), measured and modeled, were compared graphically. The quantitative bases to evaluate model performance were the root mean square error (RMSE) and mean error (ME; observations − predictions) statistics. RMSE in particular has been used as a metric for a number of studies in which model testing targeted multiple years of observations of thermal stratification (Gelda et al. 1998, 2009, 2012, O'Donnell et al. 2010).

The validated model was applied through numeric conservative tracer simulation experiments to describe and quantify various features of transport with implications for water quality modeling, including for the P-eutrophication issue. These experiments addressed (1) the residence times of the entire lake and the shelf, (2) the transport and fate of seasonally negatively buoyant streams, and (3) the extent of transport from the hypolimnion to the epilimnion.

To characterize the residence time of stream inputs within the shelf, passive tracers were released instantaneously in the stream once per week for the January 1994–October 2013 period (1033 experiments). The predicted

time series of the mass of the tracer remaining on the shelf (defined by the 6 m isobaths at its northern boundary) for each experiment was analyzed to determine the *e*-folding time (τ_{e1}) that corresponds to 37% of the original deployed mass remaining. The τ_{e1} values were compared to V/Q for the shelf; these would be equivalent if the shelf was well-mixed and tributaries were its only input. Similar experiments were conducted to characterize residence time of stream water within the entire lake, but tracers were instead released every 4 weeks during 1994–2002 (118 experiments).

A numerical tracer experiment was conducted to determine the fate of negatively buoyant streams by releasing a conservative tracer in the streams at noon on 4 October 2013 and tracking its fate on the shelf and lake-wide. In a second experiment, the signature of a plunged (metalimnetic maximum) turbid plume observed on 12 August 2013 at site 3 was used to initialize conservative tracer concentrations in the corresponding model segment. Tracer concentration was initialized at zero through the rest of the lake, and lake-wide concentrations were tracked functions of depth for the following week.

To determine the extent to which hypolimnetic constituents are transported to the epilimnion during the stratified period, conservative tracers were released (numeric simulation experiments) instantaneously at site 5 at 4 depths (17, 27, 40, and 60 m) on 4 days (7 May, 1 June, 1 July, and 1 August 2012), totaling 16 releases. The concentration of each tracer within the 0–13 m depth range (a reasonable proxy for the epilimnion) was tracked for 3 months.

Results

Calibration performance

Model simulations successfully reproduced temperature observations for the calibration year 2013 over the various temporal and spatial measurement scales (Fig. 2, 3a, 4b, 5, and 6). The predicted profiles successfully captured the temporal progression of stratification, including its onset, the temperatures of the layers, and the deepening of the epilimnion in early fall, as shown for the mid-lake site 5 (Fig. 2), with average RMSE and ME of 0.64 and 0.32 °C, respectively (Table 3). The respective averages for all 9 sites were 0.89 and 0.29 °C (Table 3). The seasonal near-surface temperature pattern at site 2 was also successfully simulated, (Fig. 3a). The abrupt decreases in temperature values that occurred irregularly in 2013 (e.g., early July and September; Fig. 3a) are signatures of upwelling from seiche activity (Effler et al. 2010). The timing of these events and their magnitudes were well simulated.

Color contours of vertical temperature profile time histories from the thermistor chain data (Fig. 4a) reflect dynamics at time scales extending from days to seasons. The seasonal features are recurring, depicting the onset and development of strong stratification (maximum in July and August) and its subsequent waning in fall. The more compelling feature of this representation is the high frequency dynamics of the temperatures in the stratified layers (Fig. 4a), which are clear manifestations of seiche activity (Lemmin and Mortimer 1986, Imboden 2004). The influence of these oscillations extended to depths of ~60 m in multiple cases over the monitored interval. Model simulations performed well qualitatively, representing both the timing (phase) and magnitude of these dynamics, as reflected in the same contour format (Fig. 4b).

Comparison of time series of observations with predictions of temperature at 2 stratified depths (Fig. 5a and b) provides a more rigorous test of the model's performance in representing these oscillations. The model performed well in simulating the timing (phase) and magnitude of this seiche activity. The RMSEs for the June–September interval of 2013 at metalimnetic depths of 17 m (Fig. 5a) and 27 m (Fig. 5b) were 1.8 and 1.0 °C, respectively. The vertical distribution of the average RMSE values for the June–September interval of 2013 (Fig. 5c) demonstrated a metalimnetic maximum, where strong temperature gradients prevailed, with progressive decreases through the hypolimnetic deployment depths that extended down to ~60 m. The good performance of the model related to seiche

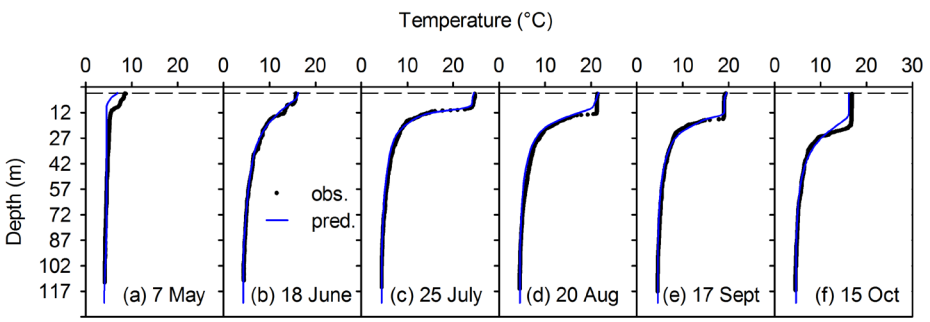

Fig. 2. Performance of 2-D hydrothermal/transport model (W2/T) in predicting monthly temperature (T) profiles at site 5 in Cayuga Lake in 2013; predictions are compared with observations. Performance statistics in Table 3.

© International Society of Limnology 2015 DOI: 10.5268/IW-5.4.804

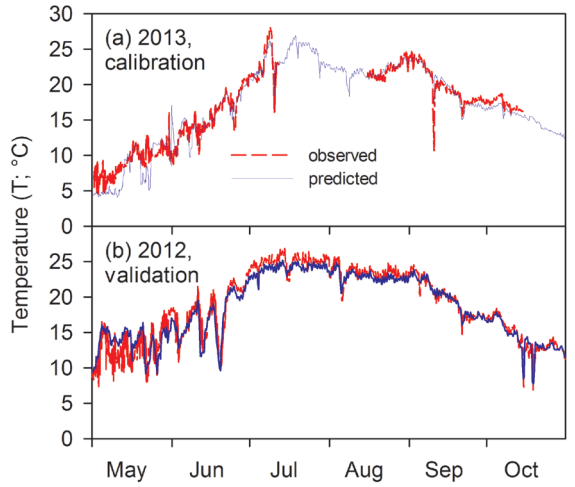

Fig. 3. Performance of 2-D hydrothermal/transport model (W2/T) in predicting surface water temperature (T) measured at the southern end of Cayuga Lake for the May–October interval: (a) 2013, calibration; and (b) 2012, validation. Performance statistics in Table 3.

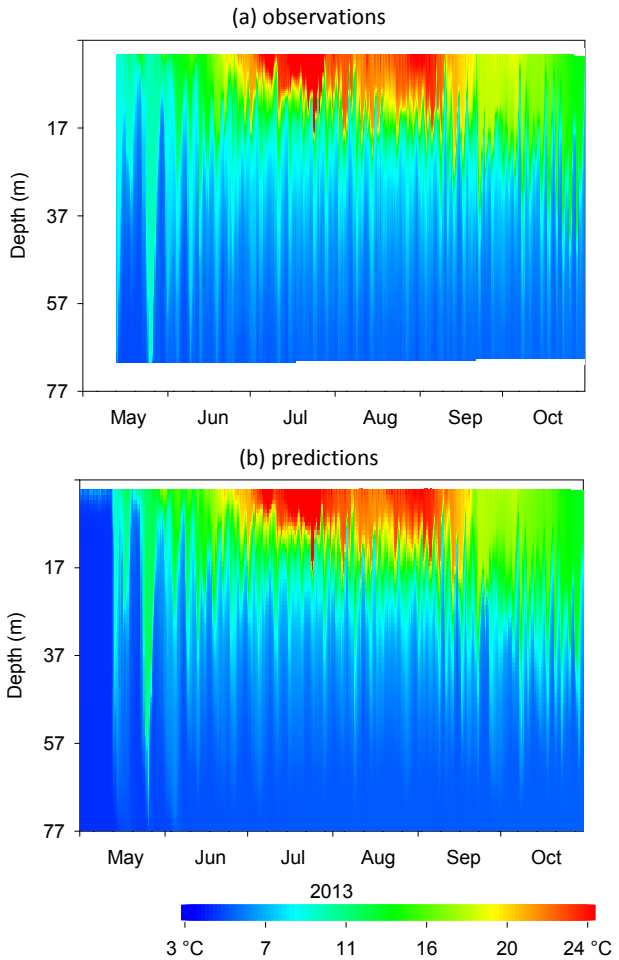

Fig. 4. Contours of vertical temperature (T) profile time series at LSC intake site, demonstrating short-term dynamics in T for the May–October interval of 2013: (a) thermistor chain observations, and (b) predictions of a 2-D hydrothermal/transport model (W2/T).

activity was also manifested in the power spectrum of temperature (e.g., Horn et al. 1986). The dominant periods of the model simulations for a depth of 17 m (5.3 and 3.3 d; Fig. 6b) closely matched those calculated from the thermistor observations (5.1 and 3.3 d; Fig. 6a). The dominant periods correspond to the mode 1 internal seiche predicted by Merian's formula (with reduced gravity based on a 2-layer characterization of observed stratification; e.g., Mortimer 1953) in early June and the first half of July, respectively.

Finally, the model simulated the modest decreases in SC observed in the upper waters at site 3, relative to spring turnover conditions (Fig. 7a and b), in response to seasonally lower levels in the southern tributaries (a dilution effect from elevated runoff; e.g., O'Donnell et al. 2011). These simulations are a valuable test of the general consistency of predicted tributary transport, mostly to the upper waters, for that interval. Plunging to the metalimnion occurs seasonally in fall and is subsequently considered.

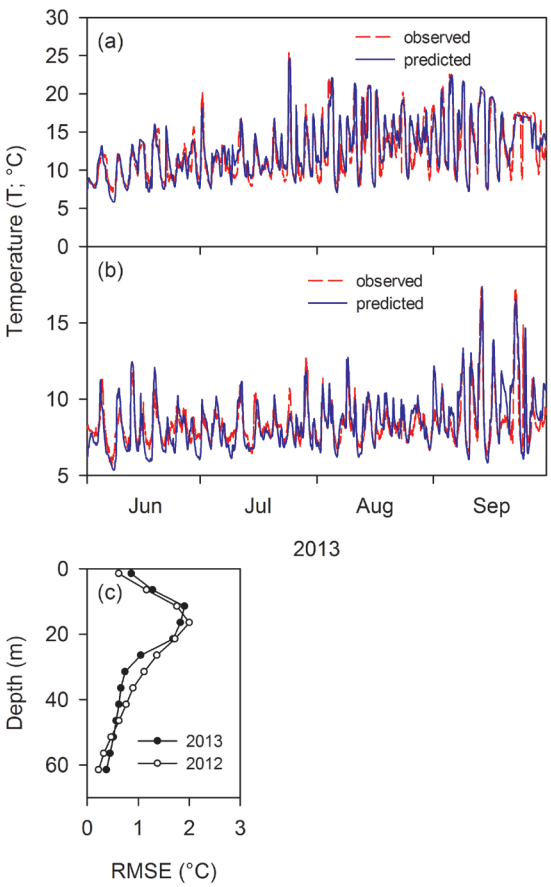

Fig. 5. Performance of 2-D hydrothermal/transport model (W2/T) in predicting temperature (T) dynamics at stratified depths in Cayuga Lake for the June–September interval of 2013: (a) depth of 17 m, and (b) depth of 27 m. Performance statistics in Table 3. Vertical profiles of the performance statistics of the root mean square error (RMSE) for thermistor deployment depths in 2012 and 2013 as (c).

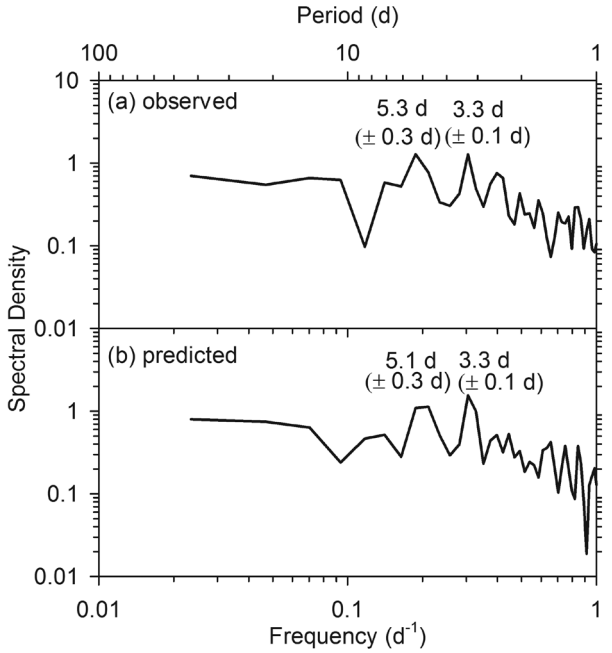

Fig. 6. Spectral analysis of temperature dynamics in Cayuga Lake at a depth of 17 m over the 1 June–mid-July interval of 2013, with dominant periods identified: (a) thermistor observations, and (b) predictions of a 2-D hydrothermal/transport model (W2/T).

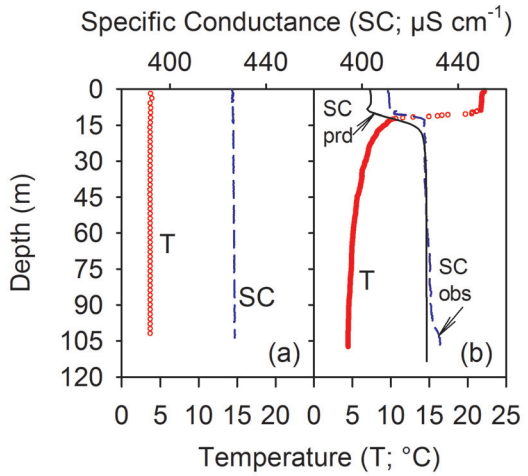

Fig. 7. Approximate predictions of the vertical distribution of specific conductance (SC) in the upper waters of Cayuga Lake at site 3 on 6 August 2013: (a) SC and temperature (T) profiles observed at site 3 during spring turnover, and (b) observed T and SC profiles and predicted SC profile at site 3 on 6 August 2013.

Validation performance

The model continued to perform well in validation testing (Tables 3–5), although some diminishment was noted prior to 2012, when only land-based meteorological measurements were available (Fig. 1, Table 2a). The performance of predictions for the thermistor chain data of 2012 (Table 2b) was similar to that reported for 2013

Table 3. Performance of the 2-D model W2/T in simulating temperature patterns in Cayuga Lake in 2013 (model calibration) and in 2012 (model validation) for near-surface waters, profiles at multiple sites, and thermistor chains.

Interval	Site*	RMSE	ME
2013			
Jun–Sep	A	1.14	−0.03
Jan–Dec	A	1.44	0.31
Apr–Oct	1	1.04	−0.08
Apr–Oct	2	0.89	0.15
Apr–Oct	3	0.84	0.16
Apr–Oct	4	0.63	0.29
Apr–Oct	5	0.64	0.32
Apr–Oct	6	0.55	0.13
Apr–Oct	7	0.76	0.25
Apr–Oct	8	1.31	0.80
Apr–Oct	9	1.38	1.01
Jun–Sep	LSC In.	0.96+	0.06+
Jun–Sep	LSC In.	0.38–1.9++	−0.45–0.33++
2012			
Jun–Sep	A	0.96	0.53
Jan–Dec	A	1.43	0.12
Jun–Sep	LSC In.	0.94+	−0.36+
Jun–Sep	LSC In.	0.18-2.0++	−0.67–0.12++

* site A: near-surface thermistor, sites 1–9: temperature profiles, LSC In.: thermistor string
+ average
++ range for depths

(Fig. 5c, Table 3; see LSC In., Fig 1). The RMSE and ME for the near surface temperatures of the southern end of the lake for the May–October interval in 2012 (Fig. 3b) were 1.24 and 0.26 °C, respectively.

Near-surface temperature at the southern end of the lake (site A) was reasonably predicted for the summer intervals for each of the other 14 years of thermistor deployment (Table 2b) over the 1998–2011 period (Table 4). The average RMSE for that period was 1.61 °C, and the range was 0.86–2.33 °C. Performance in 2012 (Fig. 3b, Table 3), when on-lake meteorological measurements were available, was particularly good. A total of 32 upwelling events (defined as ≥5 °C decrease in T within a day at site A, a definition that identifies only upwelling events strong enough to surface far along the shelf) were identified for the summer intervals of the 15 years, ranging from 1 (2007) to 6 (2004) occurrences annually. The model successfully predicted >90% of these irregularly timed events. The error in the predicted minimum

© International Society of Limnology 2015 DOI: 10.5268/IW-5.4.804

Table 4. Performance of the 2-D model W2/T in simulating near-surface temperature for 2 intervals annually for the 1998–2011 period and the effect of adjustments for off-lake meteorological measurements.

Year	Near-surface Thermistor on Shelf							
	Jun–Sep				Jan–Dec			
	Offsite Met. Data		Adj. to Onsite Met. Data		Offsite Met. Data		Adj. to Onsite Met. Data	
	RMSE	Mean Error	RMSE	Mean Error	RMSE	Mean Error	RMSE	Mean Error
1998	0.86	−0.59	0.63	−0.02	0.83	−0.45	0.62	−0.05
1999	1.55	−0.84	1.07	−0.17	1.76	−0.68	1.36	−0.19
2000	1.12	0.51	1.49	1.14	1.41	0.23	1.43	0.59
2001	1.31	−0.37	1.09	0.33	1.50	−0.19	1.18	0.18
2002	1.13	−0.44	1.17	0.34	2.03	−0.21	1.88	0.15
2003	2.13	−1.54	1.76	−0.98	2.01	−1.08	1.70	−0.76
2004	2.33	−1.85	1.95	−1.25	2.35	−1.37	2.03	−0.96
2005	2.06	−1.00	1.89	−0.06	2.02	−0.91	1.80	−0.33
2006	1.40	0.79	1.53	1.06	1.65	0.33	1.52	0.50
2007	1.58	−0.67	1.39	−0.11	1.58	−0.40	1.52	−0.17
2008	1.59	−0.67	1.28	−0.22	1.42	−0.10	1.26	−0.15
2009	1.30	−0.68	1.19	−0.38	1.38	−0.56	1.25	−0.41
2010	1.87	−1.14	1.67	−0.76	2.20	−0.39	2.02	−0.28
2011	2.27	−1.07	1.91	−0.47	1.93	−0.59	1.78	−0.33
Avg	**1.61**	**−0.68**	**1.43**	**−0.11**	**1.72**	**−0.46**	**1.53**	**−0.16**

temperature of the upwelling event relative to the observations was ≤2 °C for 75% of the events.

Vertical profiles of temperature at site 2, the LSC intake, and site 3 over the 1998–2006 meteorological monitoring sites (Table 2b) were also reasonably simulated (Table 5). The average RMSEs over these 9 years for the 3 sites were 1.30, 1.87, and 1.65 °C, respectively. This level of performance is somewhat diminished compared to the 2013 simulation (Table 3), which was supported by on-lake meteorological measurements. Substantial differences in epilimnetic temperatures were observed over the validation period, thereby offering a robust test of the model's heat budget (e.g., average June values ranged from 12.6 °C in 2003 to 17.7 °C in 2012).

Improvements in model performance (Tables 4 and 5) were achieved for years in which only land-based meteorological measurements were available (before 2012) by adjusting land-based measurements of wind velocity with a sector-based linear transform developed from paired on-lake and land-based observations. The improvement for the near-surface temperatures on the shelf was modest based on the RMSE (Table 4); however, the relative improvement based on ME was substantial, decreasing on average 83 and 65%, respectively, for these intervals (Table 4). Noteworthy improvements in performance were also observed in predictions of temperature profiles over the 1998–2006 period by adopting the adjustment (Table 5). The RMSE decreased on average by 15, 33, and 23% for site 2, site 3, and site LSC Intake, respectively. The ME decreased (on absolute basis) by 58, 53, and 84% for these sites.

Sensitivity analyses

Sensitivity analyses were conducted for a number of specifications made as part of model testing to identify potential sources of uncertainty or bias. Predictions of short-term variations of temperature in stratified layers (e.g., Fig. 5a) were insensitive to reasonable levels (±10%) of uncertainty in the Chezy (i.e., bottom shear stress; Table 1) coefficient (±3.8% change in RMSE). Summertime predictions of temperature were insensitive to the inclusion of the representation of the partial ice-cover (north and south ends) experienced by the lake in winter in some years (not considered in the tested model; no change in RMSE). Model predictions were also insensitive to the simplifying assumption of uniform distribution of the small ungauged stream inputs versus a

Table 5. Performance of the 2-D model W2/T in simulating temperature profiles at 3 sites annually for the 1998–2006 period and the effect of adjustments for off-lake meteorological measurements.

Year	Temperature Profiles (Apr–Oct)											
	site 2				site 3				LSC Intake			
	Offsite Met. Data		Adj. to Onsite Met. Data		Offsite Met. Data		Adj. to Onsite Met. Data		Offsite Met. Data		Adj. to Onsite Met. Data	
	RMSE	ME	RMSE	ME	RMSE	ME	RMSE	ME	RMSE	ME	RMSE	ME
1998	0.99	−0.18	0.60	−0.04	2.06	0.55	1.14	−0.69	2	1.20	1.27	0.01
1999	1.36	−0.63	0.88	−0.34	1.88	0.46	1.12	−0.57	1.82	0.84	1.44	−0.02
2000	0.88	−0.14	1.07	0.23	1.71	0.80	1.23	0.17	1.14	0.36	1.15	−0.22
2001	1.92	−1.45	1.43	−1.11	1.62	−0.15	1.32	−0.89	1.65	0.11	1.37	−0.67
2002	1.24	−0.42	1.03	−0.22	2.43	1.49	1.14	0.26	1.84	1.29	1.11	0.46
2003	1.02	−0.24	1.01	−0.23	1.6	−0.19	1.36	−0.73	1.26	0.03	1.17	−0.46
2004	1.43	−0.07	1.18	−0.10	1.76	0.49	1.28	−0.15	1.7	0.62	1.40	−0.36
2005	1.29	−0.39	1.20	0.23	1.65	0.21	1.36	−0.44	1.34	0.18	1.22	−0.53
2006	1.58	−0.15	1.49	0.04	2.13	1.59	1.23	0.65	2.11	1.55	1.27	0.80
Avg	**1.30**	**−0.41**	**1.10**	**−0.17**	**1.87**	**0.58**	**1.24**	**−0.27**	**1.65**	**0.69**	**1.27**	**−0.11**

more spatially detailed specification (based on the watershed area of specific ungauged tributaries entering the shelf region; +0.5% change in RMSE).

The potential effect of the specification of the longitudinal segmentation (Fig. 1) was evaluated by reconfiguring the model grid with more segments (69 instead of 48). The effects of the finer grid on predictions (e.g., compared with predictions of Fig. 5a) were negligible (−0.5% change in RMSE), supporting the appropriateness of the adopted grid. The sensitivity of model performance to on-lake versus land-based (A vs. B; Fig. 1) meteorological drivers was evaluated for 2013 by driving the model instead with the meteorological data from site B. Diminished model performance resulted from use of the site B data; for example, the RMSE for the profiles of site 1 increased from 1.04 to 1.36 °C, while the RMSE increased for site 5 from 0.64 to 1.01 °C. This level of deterioration is similar to that reported for the validation years (driven by land-based meteorological data) based on profiles (sites 2 and 3) compared to calibration performance for the conditions of 2013 (Table 5). The similar performance of the model related to seiche activity in validation testing in 2012, when on-lake meteorological measurements were available, to that attained in calibration testing for 2013 (Fig. 5c) also supports the position that model performance is enhanced by the on-lake monitoring of meteorological drivers. Finally, the systematic improvement in model performance observed for years of land-based meteorological monitoring when the empirical adjustment for on-lake wind conditions was employed (Tables 4 and 5) establishes the benefit of the on-lake measurement of this key model driver.

Model applications

A broad distribution in the residence time (τ_{e1}) for the shelf was predicted (Fig. 8a) in response to variations in ambient drivers. The predicted mean τ_{e1} for the shelf (Fig. 8a) was almost 3 times smaller than the V/Q (= 10.5 d) computed from tributary inflow alone. In contrast, the predicted distribution of lake-wide τ_{e1} was narrow. Moreover, there was a distinct seasonality for the lake-wide τ_{e1}, with lower values for the interval when stratification prevail (Fig. 8b). The annual mean τ_{e1} was 5.5 y, with a season range of the monthly means of 5.2 y (May) to 5.8 y (January). Even for releases in January, however, considered an interval of turnover (Oglesby 1978), the mean τ_{e1} remained less than V/Q (= 8.2 y).

Predictions of the fate of a negatively buoyant stream corresponding to the conditions of 4 October 2013 are presented for several hours (Fig. 9a) and a few days (Fig. 9b) after its entry. The model predicted an initial plunging into the metalimnion (i.e., as an interflow; Martin and McCutcheon 1999). Substantial mixing was predicted both vertically and longitudinally over the subsequent 3 days, promoted by an internal seiche event. Approximately 70% of the originally plunged tracer mass was transported upward into the epilimnion over that interval. The predicted fate of the plunged plume observed on 12 August 2013 (Fig. 9c) was mostly upward transport into the epilimnion within several days (Fig. 9d), followed by a leveling-off in response to elimination of the concentration gradient. Only a small fraction (<10%) was predicted to be transported downward into the hypolimnion (Fig. 9d).

© International Society of Limnology 2015 DOI: 10.5268/IW-5.4.804

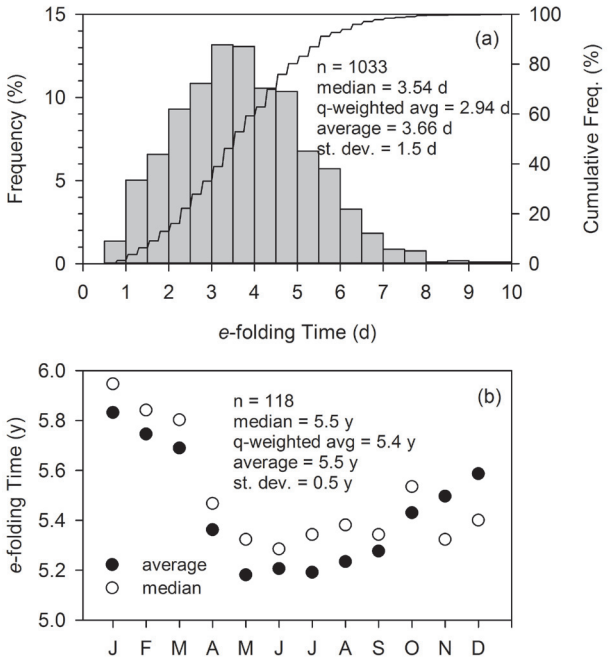

Fig. 8. Application of validated 2-D hydrothermal/transport model (W2/T) to determine residence time of tributary input within the shelf and the entire lake. (a) Shelf's *e*-folding time (time until fraction $e-1$ of the tracer mass remains), and (b) monthly mean and median *e*-folding times for the entire lake.

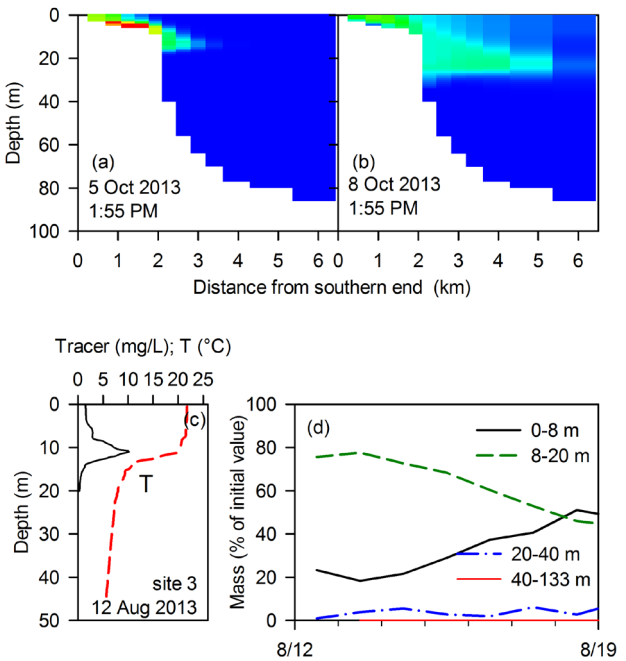

Fig. 9. Application of validated 2-D hydrothermal/transport model (W2/T) related to plunged inflows: (a) prediction of the entry of a negatively buoyant stream on 5 October 2013 as a plunging inflow, tracked as conservative tracer; (b) predicted distribution of the tracer 3 days later demonstrating substantial upward and longitudinal transport over the intervening interval; (c) plunged inflow (interflow) signature, based on observations at site 3 on 12 August 2013, used as initial tracer pattern; and (d) predicted vertical fate of the interflow over the following week.

Noteworthy net transport to the epilimnion over the following 2 month intervals from tracer additions to stratified layers was predicted to be limited to depths ≤40 m (Fig. 10a–d), similar to the observed (Fig. 4a) and predicted (Fig. 4b) depths influenced by the seiche oscillations. The results of these analyses are presented as cumulative fractions (as %) of the tracer predicted to be transported into the upper 13 m depth. The short-term peaks in the overall increasing trajectories of the transported tracer reflect effects of seiche-driven oscillations. The greatest upward transport was observed in early May (Fig. 10a) when stratification was developing. The transport from the uppermost depth considered, 17 m (positioned within the metalimnion), was in all cases the greatest of the evaluated depths, with decreases at both 27 and 40 m (Fig. 10a–d). Some delay was noted for the experiments that started in July (Fig. 10c) and August (Fig. 10d), indicating intervals of low vertical mixing.

Discussion

Performance

Performance results support both the robustness of W2/T from extensive testing and its successful performance for Cayuga Lake (Tables 3, 4, and 5). The model captured both the longer-term (seasonal and multiyear) dynamics of the thermal stratification regime (Fig. 2 and 4a) and the short-term oscillations of stratified layers associated with seiche activity (Fig. 5 and 6), particularly when on-lake wind measurements or adjustments of local land-based observations were made. The documented performance compares favorably with other efforts reported in the literature. The duration of successful simulations for pelagic waters, 11 years (1998–2006, 2012, 2013), ranks as one of the longest reported. Long-duration testing efforts were reported for several other New York systems, including Onondaga Lake, using a 1-D model (8 y: Owens 1998; later 19 y: O'Donnell et al. 2010) and several reservoirs using W2/T (7 y: Gelda et al. 1998; 14 y: Gelda and Effler 2007a; 13 y: Gelda et al. 2009; 22 y: Gelda et al. 2012). The average RMSE for the 3 sites on Cayuga Lake for the 10 years of pelagic temperature profiles (1.18 °C; Table 3, with on-lake wind adjustments) compared favorably with the other long-term simulation efforts (0.5–1.9 °C).

Performance of W2/T as applied to Cayuga Lake (Fig. 6) was consistent with 2 earlier tests of the model with respect to the convergence of predicted and observed periods of internal waves (Gelda et al. 1998, Gelda and Effler 2007a). The RMSE values for the affected stratified layers reported

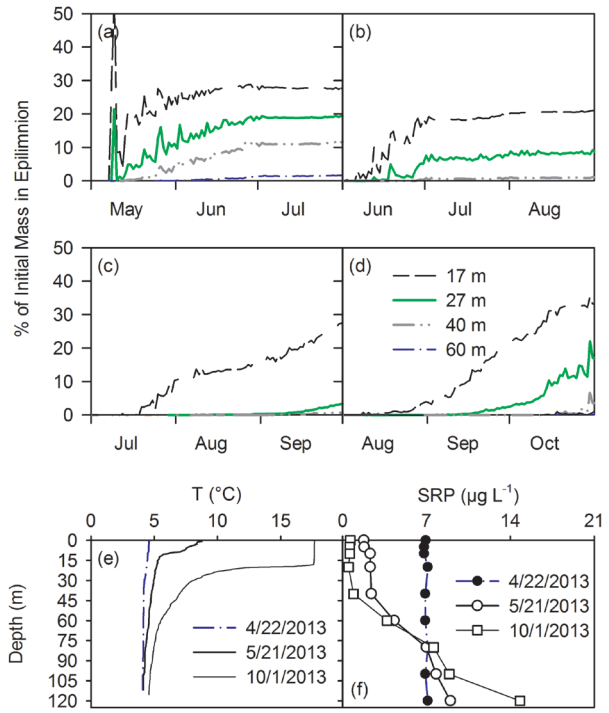

Fig. 10. Application of validated 2-D hydrothermal/transport model (W2/T) to estimate vertical transport from multiple hypolimnetic depths to the epilimnion (defined as depths between 0 and 13 m, based on 2013 T measurements) with temporal progression of upward transport for tracer inputs starting in (a) early May, (b) 1 June, (c) 1 July, and (d) 1 August.

here, also based on thermistor chain observations (Fig. 5c), represent a more rigorous test because they address both timing and magnitude. We found no previous W2/T or other 2-D model contributions to the literature reporting internal wave simulation performance based on RMSE or other error statistics. Moreover, RMSE representations of performance with respect to longer-term thermal structure are often lacking because conditions at different depths are not considered. Our analysis revealed a strong dependence of RMSE on depth (Fig. 5c), with a positive dependence of RMSE on the magnitude of the temperature variations imparted by the seiche oscillations (greatest in the metalimnion and diminished in the hypolimnion).

Recent applications of more complex 3-D models to other lakes provide a basis for comparison of model performance, although the simulation durations were substantially shorter in most cases (Rueda and Cowen 2005, Laborde et al. 2010, Okely et al. 2010, Dorostkar 2012) than the 4 months addressed here with W2/T in both 2012 and 2013 (e.g., Fig. 5). Performance of W2/T at Cayuga Lake in this regard approached that reported based on shorter-term applications of the Estuary Lake and Coastal Ocean Model (ELCOM; Hodges et al. 2000) to Valle de Bravo Reservoir, Mexico (overall average of 0.41 °C; Okely et al. 2010), and Lake Como, Italy (0.70–0.81 °C; Laborde et al. 2010), and applications of Si3D to Little Sodus Bay (overall average 0.63 °C; Rueda and Cowen 2005). A more direct comparison with the performance of a 3-D model (MIT general circulation model) can be made for Cayuga Lake (Dorostkar and Boegman 2013), for which a detailed vertical profile of RMSE was also reported based on an 11 d simulation interval (Dorostkar 2012). The performance of W2/T generally compared favorably; the RMSE values for W2/T and this 3-D model (Dorostkar 2012) were 1.8 and 2.7 °C for a depth of about 18 m, and 0.5 and 0.4 °C at 50 m, respectively.

The third element of robust of testing of W2/T for Cayuga Lake was the successful simulation for 16 y of the summertime near-surface temperature dynamics for the southern end of the lake (Table 4) that included the irregular occurrences of upwelling events. We are unaware of similar long-term testing of a 2-D model for surface waters (here the shelf) featuring upwelling events.

Applicability and transferability

Other successful multiple year testings of W2/T have been reported in the peer-reviewed literature, primarily for high aspect ratio reservoirs (e.g., Gelda et al. 1998, 2009, 2012, Gelda and Effler 2007a). Boegman et al. (2001) reported what they described as the first successful testing of W2/T for a large natural lake, Lake Erie; however, even though Lake Erie's aspect ratio is 6:1, substantial modification of W2/T's "vertical mixing algorithm was required to suppress excessive low frequency wind forced oscillations" (Boegman et al. 2001, p. 868) to achieve validation. These modifications were in large part associated with the large width of that lake (>100 km), and the lateral transport induced by Coriolis likely played a roll (Boegman et al. 2001). The Cayuga Lake application reported here represents a second successful testing of W2/T for a natural lake that certainly qualifies for the "large" description compared to most inland lacustrine systems, although it is much smaller than Lake Erie. The major difference in these two W2/T applications is the high performance of W2/T for Cayuga Lake without modifications in the fundamental mixing algorithms, apparently attributable to its much narrower width (maximum of 5.3 km; Fig. 1). An objective threshold of width is not currently available, for which no modification of this model's mixing algorithms is necessary, but Boegman et al. (2001) provided some valuable insight, identifying the internal Rossby radius of deformation associated with the onset of Coriolis influences as a likely relevant lateral length scale. Lake Erie is an order of magnitude or more wider than its internal Rossby radius, and Coriolis forces are dominant.

© International Society of Limnology 2015 DOI: 10.5268/IW-5.4.804

The Burger number (S) has been identified as the single critical parameter controlling the internal wave frequency response in a lake affected by the earth's rotation (Antenucci and Imberger 2001). The Burger number can be considered as the ratio of the internal Rossby radius to the basin width. Rotation signatures (e.g., Kelvin waves) can be resolved for $S < 1$, although there is no sharp cutoff. Instead, gradual changes in the character of internal waves occur as S decreases in this range. Kelvin waves were reported in Kootenay Lake associated with weak cross-lake thermocline tilt (Hamblin and Carmack 1978), where S was ~1 (Antenucci 2005). Given the range of Burger numbers for Cayuga Lake (0.4–1.9), there may be intervals when internal waves are influenced by rotation. The earth's rotation was found to be important in Lake Kinneret, which has a substantially "rounder" configuration, where S was ~0.7 (Antenucci and Imberger 2003). Such an influence apparently is not large enough to substantially degrade the performance of the 2-D model for Cayuga Lake (e.g., Tables 3, 4, and 5), a framework that cannot represent the effects of rotation.

There are a large number of high aspect ratio lacustrine systems for which application of W2/T, without modification, should be successful. For example, W2/T is likely appropriate for most of the other 10 New York Finger Lakes (Fig. 1). Applications for other lakes with Burger numbers shifted lower (but not much lower) than for Cayuga Lake are recommended to objectively identify a threshold for appropriate applications without modification. Moreover, the model coefficient values (Table 1) for successful validation have not been found to differ greatly for the various narrow, high aspect ratio systems for which it has been tested (Gelda et al. 1998, 2009, 2012, 2013, Gelda and Effler 2007a). The primary differences have been for the longitudinal eddy diffusivity (range 1–10 $m^2\ s^{-1}$) and wind sheltering coefficients. The sheltering coefficient value has been qualitatively consistent with the surrounding topographies of the specific basins addressed (value decreases with greater sheltering).

Application of W2/T for Cayuga Lake

Two-dimensional W2/T is an appropriate and parsimonious choice as the transport submodel for water quality models for Cayuga Lake, including one focused on the P-eutrophication issue. A 1-D model (e.g., O'Donnell et al. 2010) would not be an appropriate selection because of the established longitudinal differences in water quality, which is a management issue, and prominence of seiche activity in the transport regime of the lake (Effler et al. 2010). The longitudinal differences reported for water quality for the lake in part reflect the localized entry of a large fraction of external constituent loading at the south end (Effler et al. 2010), a situation common to many reservoirs (Thornton et al. 1990). The wide time-scale capabilities of W2/T are consistent with the needs of water quality models. This framework represents the effects of both short-term hydrologic and wind events and seasonal dynamics in response to drivers, and it can be used, as demonstrated here (Table 4 and 5), to create multiyear (long-term) simulations. Elsewhere, W2/T has served as the transport submodel to predict (1) 2-D patterns of turbidity plumes formed from particle inputs delivered during rainfall/runoff events in water supply reservoirs (Gelda and Effler 2007b, Gelda et al. 2009, 2012, 2013), (2) transport and fate of spills of a toxic chemical along the axis of a water supply reservoir (Chung and Gu 1998), and (3) the seasonal dynamics and spatial patterns of phytoplankton growth in a eutrophic system in response to the dynamics and positions of nutrient loading (Doerr et al. 1998). The stability of W2/T to make credible longer-term (multiyear) simulations of the hydrothermal and transport regimes, together with long-term datasets of hydrologic and meteorological drivers, has enabled multiyear projections elsewhere (Gelda and Effler 2008). This approach is valuable to managers by providing a probabilistic context for predictions that reflect the often important effects of natural variations in these drivers (Gelda and Effler 2008).

Boegman et al. (2008a, 2008b) documented the critical role W2/T played in a water quality (P-eutrophication) model for Lake Erie in representing the influence of dreissenid mussels. The metabolic effects of grazing and excretion by these benthic organisms were demonstrated to be substantially attenuated much of the time relative to the upper-bound values reported from well-mixed laboratory experiments (Boegman et al. 2008a, 2008b). This attenuation was attributed to the formation of a concentration boundary layer of thickness ~1 m during intervals of low ambient mixing. The simulation of the dynamics of ambient mixing in Lake Erie with W2/T served to specify the attendant dynamics of this attenuating effect and the associated mussel fluxes in the overall water quality model (Boegman et al. 2008a, 2008b). This approach, implemented through W2/T, will be valuable in representing the effects of the dense mussel populations of Cayuga Lake (Watkins et al. 2012) in a forthcoming water quality model for the lake.

Three-dimensional models are necessary where detailed lateral (as well as vertical and longitudinal) resolution is required. Lateral differences in certain water quality metrics (e.g., turbidity) occur irregularly on the shelf (Effler et al. 2010), and ongoing development of a 3-D model will support investigation of this transient lateral heterogeneity and provide further validity tests of the W2/T 2-D framework for certain applications, including shelf residence time and fate of negatively

buoyant inflows. Lateral heterogeneity, however, does not persist at the temporal and spatial scales of interest associated with Cayuga Lake's P-eutrophication issues. A 3-D transport submodel is not a parsimonious choice for a water quality model for this lake. Moreover, continuous simulations for multiple (e.g., ≥10 y) years with a 3-D transport submodel have yet to be reported.

The applications of W2/T to Cayuga Lake reported here are valuable in the context of describing the interplay between transport processes and certain features of water quality. Residence time has been described as a first-order representation of the transport regime of lacustrine systems and a key regulating parameter of a system's biogeochemical behavior (Rueda et al. 2006). The low predicted mean residence time for the shelf (τ_{e1} = 3.7 d; Fig. 8a), relative to the completely mixed assumption estimate (V/Q = 10.5 d, which accommodated only the tributary inflow to this portion of the lake) established that exchange with the greater lake basin, driven by mixing processes (e.g., seiche activity), contributes importantly to flushing of the shelf. Accordingly, natural variations in meteorological conditions, particularly wind, and hydrologic conditions contribute to the predicted variability in τ_{e1} (Fig. 8a). The relatively low residence time (e.g., high flushing rate; d^{-1}) is an important factor in the lack of localized high phytoplankton biomass concentrations on the shelf, despite higher nutrient concentrations (Effler et al. 2010). The flushing rate is substantial (Effler et al. 2010) relative to net phytoplankton growth rates (Chapra 1997, Reynolds 2006). The e-folding residence time of tributary inputs within the entire lake based on the tracer analysis (5.5 y; Fig. 8b) was substantially shorter than the completely mixed lake assumption value (V/Q = 8.2 y). While the annual stratification regime (~6 months) is one factor contributing seasonally to incomplete mixing (Fig. 8b), other features, such as intervals of limited vertical mixing during non-stratified periods, also may diminish the effective residence time compared with the completely mixed case. Regardless of these differences, the residence time of this lake is relatively long, indicating the important role lake metabolism versus watershed inputs can be expected to play in regulating biogeochemical signatures within most of the lake (Rueda et al. 2006).

Plunging of negatively buoyant tributaries to metalimnetic depths, particularly on a seasonal basis, has been reported widely (Romero and Imberger 2003, Effler et al. 2009) and occurs in more lacustrine systems than currently recognized. For example, the negative buoyancy of the stream, based on temperature observations for the date in early October 2013, occurs widely in north temperate climates (e.g., Gelda and Effler 2007b, Gelda et al. 2009, 2013, O'Donnell et al. 2011) when streams cool more rapidly than the epilimnion (Martin and McCutcheon 1999). The occurrence of plunging in Cayuga Lake seasonally was manifested in both observations and W2/T simulations (Fig. 9). Despite the effects of ambient mixing in redistributing these interflows (Fig. 9), these transport processes, including the initial plunging, can be important in a water quality context. For example, the routing of enriched inflows to stratified depths diminishes the effective loading from these sources to the productive upper waters (Romero and Imberger 2003, Effler et al. 2009). The magnitude of this effect depends on the rates of loss or transformation of the constituent of interest within the interflow layer relative to the rate of upward transport to the epilimnion (Owens et al. 2013). W2/T has been reported to perform well in predicting the timing and 2-D patterns associated with the plunging phenomenon elsewhere (Gelda and Effler 2007b, Gelda et al. 2009, 2013, O'Donnell et al. 2011), supporting the representativeness of the predictions of the transport and fate of negatively buoyant inflows and associated interflow plumes presented here for Cayuga Lake.

Upward vertical transport to productive epilimnia from enriched hypolimnia has been recognized by the water quality modeling community as a potentially critical recycling pathway in many cases (Chapra 1997). The results of the vertical transport analyses for a conservative tracer conducted with W2/T (Fig. 10a–d) provided insights relative to the transport of solutes. Upward transport of solutes from the deepest portions of the hypolimnion during summer stratification was predicted to be minor for this deep lake but was substantial for metalimnetic depths.

The factors that contribute to making W2/T an appropriate transport submodel for a water quality model for Cayuga Lake include (1) the basin morphology and associated transport characteristics, (2) longitudinal differences in water quality metrics imparted from localized inputs, and (3) the demonstrated performance of W2/T in representing transport in this lake across multiple time scales. These lake characteristics and concerns for representation of spatial patterns are broadly occurring, making W2/T an appropriate transport submodel for many water quality modeling initiatives. Its successful application in supporting the representation of the effects of dreissenids mussel metabolism (Boegman et al. 2008a, 2008b) makes it a particularly attractive choice in North America where these invaders are having major effects (Nalepa and Schlosser 2014).

Acknowledgements

Funding was provided by Cornell University. This is contribution number 327 of the Upstate Freshwater Institute.

© International Society of Limnology 2015 DOI: 10.5268/IW-5.4.804

References

Antenucci JP. 2005. Comment on "Are there internal Kelvin waves in Lake Tanganyika" by Jaya Naithani and Eric Deleersnijder. Geophys Res Lett. 32.

Antenucci JP, Imberger JA. 2001. Energetics of long internal gravity waves in large lakes. Limnol Oceanogr. 46:1760–1773.

Antenucci JP, Imberger JA. 2003. The seasonal evolution of wind/internal wave resonance in Lake Kinneret. Limnol Oceanogr. 48:2055–2061.

Boegman L, Loewen MR, Hamblin PF, Culver DA. 2001. Application of a two-dimensional hydrodynamic reservoir model to Lake Erie. Can J Fish Aquat Sci. 58:858–869.

Boegman L, Loewen MR, Hamblin PF, Culver DA. 2008a. Vertical mixing and weak stratification over zebra mussel colonies in western Lake Erie. Limnol Oceanogr. 53:1093.

Boegman L, Loewen MR, Culver DA, Hamblin PF, Charlton MN. 2008b. Spatial-dynamic modeling of algal biomass in Lake Erie: relative impacts of dreissenid mussels and nutrient loads. J Environ Eng. 134:456–468.

Bootsma HA, Liao Q. 2014. Nutrient cycling by Dreissenid mussels: controlling factors and ecosystem response (Chapter 35). In: Nalepa TF, Schloesser DW, editors. Quagga and zebra mussels: biology, impacts, and control, 2nd ed. Boca Raton (FL): CRC Press, Taylor & Francis Group. 775 p.

Chapra SC. 1997. Surface water-quality modeling. New York: McGraw-Hill. 844 p.

Cheng RT, Casulli V, Gartner JW. 1993. Tidal, Residual, Intertidal Mudflat (TRIM) Model and its applications to San Francisco Bay, California. Estuar Coast Shelf Sci. 36(3):235–280.

Chung SW, Gu R. 1998. Two-dimensional simulations of contaminant currents in stratified reservoir. J Hydraul Eng. 124:704–711.

Cole TM, Wells SA. 2013. CE-QUAL-W2: a two-dimensional, laterally averaged, hydrodynamic and water quality model, version 3.71. Portland (OR): Portland State University, Department of Civil and Environmental Engineering.

Csanady FT. 1973. Wind-induced barotropic motions in long lakes. J Phys Oceanogr. 3:429–438.

Doerr SM, Owens EM, Gelda RK, Auer MT, Effler SW. 1998. Development and testing of a nutrient-phytoplankton model for Cannonsville Reservoir. Lake Reserv Manage. 14:301–321.

Dorostkar AA. 2012. Three-dimensional dynamics of nonlinear internal waves [Ph.D. dissertation]. [Kingston, Ontario (Canada)]: Queen's University, Department of Civil Engineering.

Dorostkar, A. Boegman L. 2013. Internal hydraulic jumps in a long narrow lake. Limnol. Oceanogr. 58:153–172.

Edinger JE, Buchak EM. 1975. A hydrodynamic, two-dimensional reservoir model: the computational basis. Prepared for US Army Engineer Division, Ohio River, Cincinnati, OH. 94 p.

Effler SW, Auer MT, Johnson NA. 1989. Modeling Cl concentration in Cayuga Lake, USA. Water Air Soil Pollut. 44:347–362.

Effler SW, O'Donnell SM, Prestigiacomo AR, O'Donnell DM, Matthews DA, Owens EM, Effler AJP. 2009. Tributary plunging in an urban lake (Onondaga Lake): drivers, signatures, and implications. J Am Wat Resour Assoc. 45:1127–1141.

Effler SW, Owens EM, Schimel KA, Dobi J. 1986. Weather-based variations in thermal stratification. J Hydraul Eng. 112:159–165.

Effler SW, Prestigiacomo AR, Matthews DA, Gelda RK, Peng F, Cowen EA, Schweitzer SA. 2010. Tripton, trophic state metrics, and near-shore versus pelagic zone responses to external loads in Cayuga Lake, New York. Fund Appl Limnol. 178:1–15.

Effler SW, Prestigiacomo AR, Peng F, Gelda RK, Matthews DA. 2014. Partitioning the contributions of minerogenic particles and bioseston to particulate phosphorus and turbidity. Inland Waters. 2:179–192.

Effler AJP, Strait CM, Effler SW, Perkins MG, Prestigiacomo AR, Schulz KL. 2015. Linking CDOM patterns in Cayuga Lake, New York, USA, to terrigenous inputs. Inland Waters. 5:355–370.

Gelda RK, Effler SW. 2007a. Testing and application of a two-dimensional hydrothermal model for a water supply reservoir: implications of sedimentation. J Environ Eng Sci. 6:73–84.

Gelda RK, Effler SW. 2007b. Modeling turbidity in a water supply reservoir: advancements and issues. J Environ Eng. 133:139–148.

Gelda RK, Effler SW. 2008. Probabilistic model for temperature and turbidity in a reservoir withdrawal. Lake Reserv Manage. 24:219–230.

Gelda RK, Effler SW, Peng F. 2012. Modeling turbidity and the effects of alum application for a water supply reservoir. J Environ Eng. 138:38–47.

Gelda RK, Effler SW, Peng F, Owens EM, Pierson DC. 2009. Turbidity model for Ashokan Reservoir, New York: case study. J Environ Eng. 135:885–895.

Gelda RK, Effler SW, Prestigiacomo AR, Peng F, Effler AJP, Wagner BA, Perkins MG, O'Donnell DM, O'Donnell SM, Pierson DC. 2013. Characterizations and modeling of turbidity in a water supply reservoir following an extreme runoff event. Inland Waters. 3:377–390.

Gelda RK, Owens EM, Effler SW. 1998. Calibration, verification, and an application of a two-dimensional hydrothermal model [CE-QUAL-W2(t)] for Cannonsville Reservoir. Lake Reserv Manage. 14:186–196.

Gloor M, Wuest A, Munnich M. 1994. Benthic boundary mixing and resuspension induced by internal seiches. Hydrobiologia. 284:59–68.

Gu R, Chung SW. 1998. Reservoir flow sensitivity to inflow and ambient parameters. J Water Resour Plann Manage Div ASCE. 124:119–128.

Haith DA, Hollingshead N, Bell ML, Kreszewski SW, Morey SJ. 2012. Nutrient loads to Cayuga Lake, New York: watershed modeling on a budget. J Water Resour Plann Manage Div ASCE. 138:571–580.

Hamblin PF, Carmack EC. 1978. River-induced currents in a fjord lake. J Geophys Res. 83:885–899.

Hodges BR, Imberger J, Saggio A, Winters KB. 2000. Modeling basin-scale internal waves in a stratified lake. Limnol Oceanogr. 45:1603–1620.

Horn W, Mortimer CH, Schwab DJ. 1986. Wind-induced internal seiches in Lake Zurich, observed and modeled. Limnol Oceanogr. 31:1232–1254.

Hunkins K, Fliegel M. 1973. Internal undular surges in Seneca Lake: a natural occurrence of solitons. J Geophys Res. 78:539–548.

Imberger J. 1994. Transport processes in lakes: a review. In: Margalef R, editor. Limnology now: a paradigm of planetary problems. Amsterdam (Netherlands): Elsevier Science. p. 99–193.

Imberger J, Patterson JC. 1981. A dynamic reservoir simulation model: DYRESM 5. In: Fisher HB, editor. Transport models of inland and coastal waters. Academic Press. p. 310–361.

Imboden DM. 1990. Mixing and transport in lakes: mechanism and ecological relevance. In: Tilzer MM, Serruya C, editors. Large lakes: ecological structure and function. Berlin (Germany): Springer-Verlag. p. 47–80.

Imboden DM. 2004. The motion of lake waters (Chapter 6). In: O'Sullivan PE, Reynolds CS, editors. The lakes handbook volume 1: limnology and limnetic ecology. Malden (MA): Blackwell Publishing.

Kirk JTO. 2011. Light and photosynthesis in aquatic ecosystems, 3rd ed. New York (NY): Cambridge University Press. 662 p.

Laborde S, Antenucci JP, Copetti D, Imberger J. 2010. Inflow intrusions at multiple scales in a large temperate lake. Limnol Oceanogr. 55:1301.

Lam DCL, Schertzer WM. 1987. Lake Erie thermocline model results: comparison with 1967–1982 data and relation to anoxia occurrences. J Great Lakes Res. 13:757–769.

Lemmin U, Mortimer CH. 1986. Tests of an extension to internal seiches of Defant's procedure for determination of surface seiche characteristics of real lakes. Limnol Oceanogr. 31:1207–1231.

MacIntyre S, Jellison R. 2001. Nutrient fluxes from upwelling and enhanced turbulence at the top of the pycnocline in Mono Lake, California. Hydrobiologia. 466:13–29.

MacIsaac HJ, Sprules WG, Johannsson OE. 1992. Filtering impacts of larval and sessile zebra mussels (*Dreissena polymorpha*) in western Lake Erie. Oecologia. 92:30–39.

Martin JL, McCutcheon SC. 1999. Hydrodynamics and transport for water quality modeling. Boca Raton (FL): Lewis Publishers. 794 p.

Mortimer CH. 1953. The resonant response of stratified lakes to wind. Schweiz Z Hydrol. 15:94–151.

Nalepa TF, Pavlova V, Wong WH, Janssen J, Houghton JS, Mabrey K. 2014. Variation in the quagga mussel (*Dreissena rostriformis bugensis*) with emphasis on the deepwater morphotype in Lake Michigan (Chapter 20). In: Nalepa TF, Schloesser DW, editors. Quagga and zebra mussels: biology, impacts, and control, 2nd ed. Boca Raton (FL): CRC Press Taylor & Francis Group. 775 p.

Nalepa TF, Schloesser DW. 2014. Quagga and zebra mussels: biology, impacts, and control, 2nd ed. Boca Raton (FL): CRC Press Taylor & Francis Group. 775 p.

O'Donnell SM, Gelda RK, Effler SW, Pierson DC. 2011. Testing and application of a transport model for runoff event inputs for a water supply reservoir. J Environ Eng. 137:678–688.

O'Donnell SM, O'Donnell DM, Owens EM, Effler SW, Prestigiacomo AR, Baker DM. 2010. Variations in the stratification regime of Onondaga Lake: patterns, modeling, and implications. Fund Appl Limnol. 176:11–27.

Oglesby RT. 1978. The limnology of Cayuga Lake, In: Bloomfield JA, editor. Lakes of New York State, Volume I. Ecology of Finger Lakes. New York: Academic Press. p. 2–121.

Okely P, Imberger J, Shimizu K. 2010. Particle dispersal due to interplay of motions in the surface layer of a small reservoir. Limnol Oceanogr. 55:589.

Owens EM. 1998. Development and testing of one-dimensional hydrothermal models of Cannonsville Reservoir. Lake Reserv Manage. 14:172–185.

Owens EM, Effler SW, Matthews DA, Prestigiacomo AR. 2013. Evaluation of offshore wastewater outfall and diffuser for Onondaga Lake, NY. J Water Resour Prot. 5:1–15.

Prestigiacomo AR, Effler SW, Matthews DA, Auer MT, Downer BE, Kuczynski A, Walter MT. Forthcoming 2014. Apportionment of bioavailable phosphorus loads entering Cayuga Lake, New York. J Am Wat Resour Assoc.

Reynolds C. 2006. The ecology of phytoplankton. Cambridge (MA): Cambridge University Press. 1–436 p.

Romero JR, Imberger J. 2003. Effect of a flood underflow on reservoir water quality: data and three-dimensional modeling. Arch Hydrobiol. 157:1–25.

Rueda FJ, Cowen EA. 2005. The residence time of a freshwater embayment connected to a large lake. Limnol Oceanogr. 50:1638–1653.

Rueda F, Moreno-Ostos E, Armengol J. 2006. The residence time of river water in reservoirs. Ecol Model. 191:260–274.

Thornton KW, Kimmel BL, Payne FE. 1990. Reservoir limnology: ecological perspectives. New York (NY): John Wiley and Sons.

Vandebroek E. 2011. Development of boundary conditions and bathymetry data for modeling transport processes in the southern end of Cayuga Lake [master's thesis]. [Ithaca (NY)]: Cornell University, Engineering Division of the Graduate School.

Watkins JM, Rudstam LG, Mills EL, Teece MA. 2012. Coexistence of the native benthic amphipod *Diporeia* spp. and exotic dreissenid mussels in the New York Finger Lakes. J Great Lakes Res. 38:226–235.

Wetzel RG. 2001. Limnology: lake and reservoir ecosystems. San Diego (CA): Academic Press.

Wong WH, Holdren GC, Tietjen T, Gerstenberger S, Moore B, Turner K. 2014. Effects of invasive quagga mussels (*Dreissena rostriformis bugensis*) on chlorophyll and water clarity in Lakes Mead and Havasu of the lower Colorado River basin, 2007–2009 (Chapter 31). In: Nalepa TF, Schloesser DW, editors. Quagga and zebra mussels: biology, impacts, and control, 2nd ed. Boca Raton (FL): CRC Press Taylor & Francis Group. 775 p.

Wüest A, Lorke A. 2003. Small-scale hydrodynamics in lakes. Ann Rev Fluid Mech. 35:373–412.

Zhang H, Culver DA, Boegman L. 2008. A two-dimensional ecological model of lake Erie: Application to estimate dreissenid impacts on large lake plankton populations. Ecol Model. 214:219–241.

© International Society of Limnology 2015 DOI: 10.5268/IW-5.4.804